Water Harvesting Properties of a Zwitterionic Metal-Organic Framework

Charlene C. VanLeuven,[‡] Juby R. Varghese,[‡] Monu Joy, Fletcher B. Dix, Kyle Duell, Donald Hartman, and Mario Wriedt[*]

Department of Chemistry & Biomolecular Science, Clarkson University, Potsdam, New York 13699, United States of America, Email: mwriedt@clarkson.edu

[‡]C.C.V. and J.R.V. contributed equally to this work.

Electronic supplementary information (ESI) available: General methods, experimental procedures for MOF and ligand synthesis including ligand synthesis scheme and NMR, additional TGA data, water isotherm, crystallographic tables of MOF including refinement and geometrical parameters, and ORTEP plot. Crystal structure data has been deposited to the Cambridge Crystal Structure Database with CCDC number 2220643.

Abstract

Due to the raising scarcity of clean water in arid climates, there is an increased relevance in accessing clean and renewable water resources. One such perspective method, sorption-based atmospheric water harvesting, collects atmospheric water as an alternative to ground and surface water. Metal-organic frameworks (MOFs) are proposed as excellent porous materials for the capture and storage of small molecules, including water, owing to their large pore volume, high surface area, and chemical and structural tunability. Here a zwitterionic MOF (Ni-ZW-MOF), $[Ni(dcpb)(H_2O)_4 \cdot 14H_2O]_n$, was synthesized and studied for its water sorption performance, displaying selective water adsorption and desorption capabilities. Respective sorption properties were tested in controlled low and high humidity environments over multiple cycles, demonstrating its regenerative ability and high working capacity (126.4 mL kg^{-1} $cycle^{-1}$).

Introduction

Over 70% of the Earth's surface is covered in water, although only about 2.5% of those water sources are freshwater and even less are accessible drinking water resources.[1] As of 2020, over half of the world population experiences water stress for at least one month every year, with this number expected to continue rising.[2–4] With these problems comes the need for designing systems to provide clean renewable drinking water to water stressed areas.[5,6] Atmospheric humidity is a significant source for freshwater in both desert and tropical climates, and may be accessed through water harvesting.[7] Many methods exist for harvesting water from humid climates, including fog and solar water collectors, but high relative humidity (RH) is a requirement for efficient performance.[8,9] Arid regions often have day-night cycles of RH between 10-40%, significantly lower than necessary conditions for traditional water collectors. Previously, metal-organic

framework (MOF) adsorption-based water harvesters have been investigated for their performance in arid climates.[10–16]

MOFs are nanoporous, crystalline materials constructed from the self-assembly of metal ions or clusters and polytopic organic ligands. MOFs were first reported before the start of the 21st century, and have since gained traction due to their advanced performance in adsorption applications.[17,18] This enhanced performance is due to their high internal surface areas and pore volumes in addition to their customizable structures from the large availability of metal-ligand combinations. Many water stable MOFs have been previously reported for their water harvesting potential, but zwitterionic ligand-based MOFs have yet to be investigated for their water adsorption performance.[19–22]

Zwitterions are molecules featuring both positive and negative charges from present functional groups (e.g., pyridinium and carboxylates).[23,24] If used for MOF synthesis, these ligands can generate charged-polarized pore environments which have the potential to induce strong host-guest interactions of polarizable guest molecules. For example, bipyridinium-based carboxylate ligands possess quaternary ammonium salts which can act as Lewis acid sites, increasing affinity for adsorption of water molecules.

In this work, a nickel-based zwitterionic MOF, $[Ni(dcpb)(H_2O)_4 \cdot 14H_2O]_n$ (Ni-ZW-MOF), composed of a tetratopic bipyridinium carboxylate ligand ($H_4dcpb \cdot 2Cl$ = 1,1'-bis(3,5-dicarboxyphenyl)-4,4'-bipyridinium dichloride) featuring accessible hydrogen bonding sites and coordinated and non-coordinated water molecules, is studied for its water sorption performance in arid and humid environments. The activated MOF possesses two Lewis acid sites which includes a node-based open Ni^{2+} site and a ligand-based pyridinium moiety and exhibits hydrochromic behavior providing visual indication of the water harvesting process. Static and dynamic water

adsorption experiments were conducted to investigate the Ni-ZW-MOF's ability to harvest water from air in low and high humidity conditions.

Results and Discussion

Crystals of Ni-ZW-MOF were obtained from a reaction of $Ni(ClO_4)_2 \cdot 6H_2O$ and the ZW ligand H_4dcpb·2Cl in an equivalent mixture of DMF/H_2O using dicyandiamide as a modulator. Experimental details of the MOF and ligand synthesis are provided in the Supporting Information. Single crystal X-ray diffraction analysis revealed that Ni-ZW-MOF crystallizes in the monoclinic space group *C*2/c with the asymmetric unit composed of a half Ni(II) metal center, half dcpb ligand, two coordinated water molecules, and seven lattice water molecules. **Figure S2** displays the corresponding ORTEP plot at 50% electron density probability level. The Ni(II) centers are octahedrally coordinated by six O atoms of two monodentate dcpb ligands and four water molecules (**Figure 1a**). These octahedral nodes are bridged by dcpb ligands into 1D zigzag chains which are represented in **Figures 1b** and **1c** along the crystallographic *b*- and *c*-axis, respectively. Non-coordinating carboxyl groups of the dcpb ligand allow lattice water molecules to interconnect those chains through hydrogen bonding interactions into a 3D supramolecular framework. Respective hydrogen bonds are listed in **Table S7**. This structural arrangement results into the formation of 1D channel pores (9.6 x 11.5 $Å^2$) along the crystallographic *b*-axis which are filled by 14 non-coordinating lattice water molecules per formula unit as shown in **Figure 1d**.

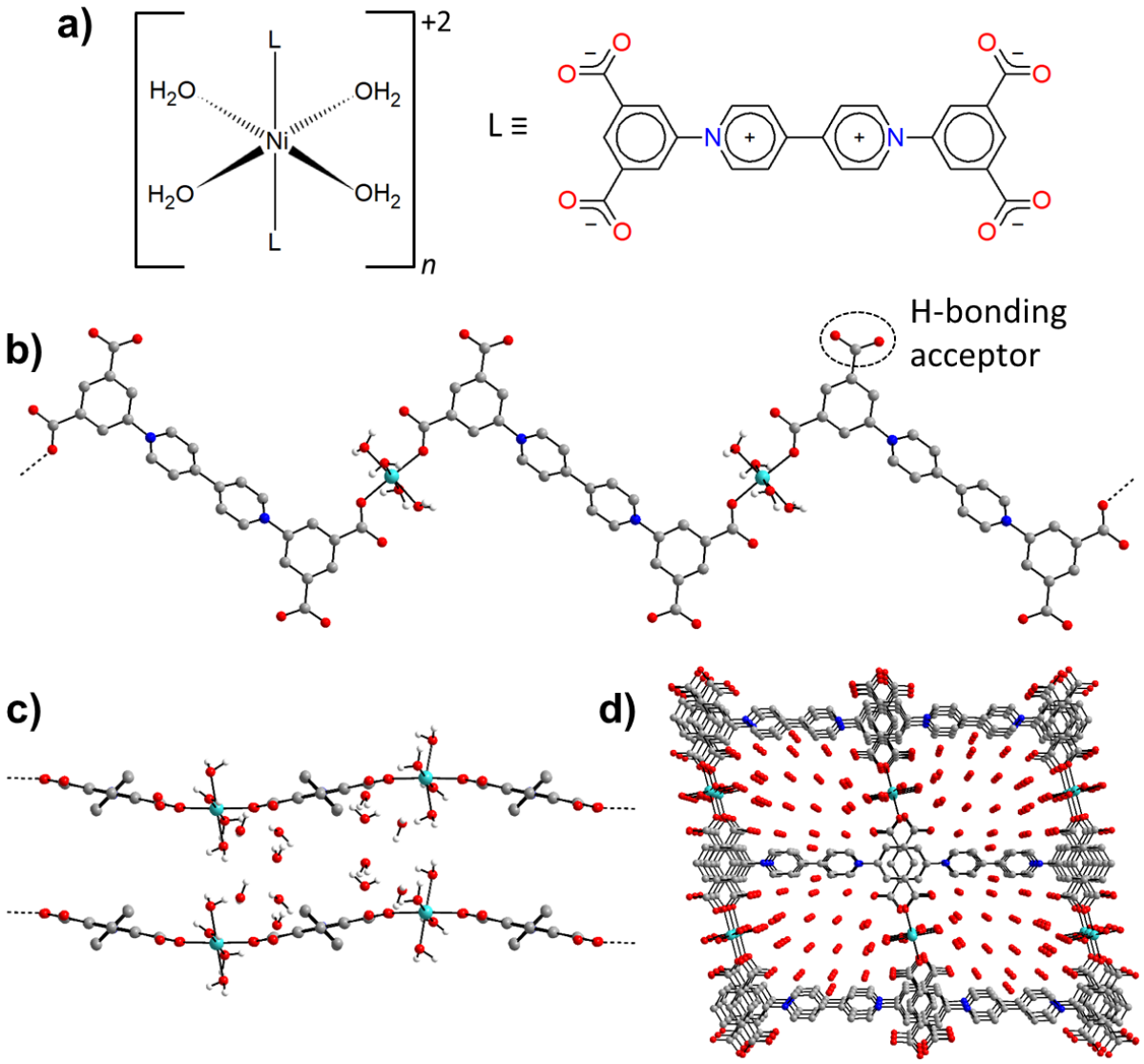

Figure 1. Crystal structure of Ni-ZW-MOF. a) Octahedral coordination environment of Ni^{2+} cations with L representing the ZW ligand dcpb; 1D zigzag chains shown along the crystallographic b) *b*-axis and c) *c*-axis; and d) Packing diagram along the crystallographic *b*-axis. Aromatic hydrogens and disorder are omitted for clarity; grey-carbon, blue-nitrogen, red-oxygen, cyan-nickel.

The thermal behavior of Ni-ZW-MOF was investigated using thermal gravimetric analysis (TGA) under a nitrogen atmosphere. From the full temperature profile ranging 20-800 °C as shown in **Figure 2a** it is evident that the MOF dehydrates upon heating to 100 °C followed by decomposition starting around 300 °C. The initial mass loss step totals around Δm_{exp}(20→100 °C) = 29.3% which is less than one would expect for the removal of 18 water molecules as calculated from SCXRD data Δm_{cal}(-18 H_2O) = 38.0%. This deviation is no surprise given that some volatile lattice water molecules might have evaporated during vacuum filtration of the sample in preparation for the TGA measurement. The initial heating step can be separated into two consecutive events on closer examination of the <100 °C region as detailed in **Figure 2b**. The first derivative of the TGA curve is also plotted as reference to indicate the inflection points of each step in the dehydration process. The first step with Δm_{exp}(20→60 °C) = 20.5% and second step with Δm_{exp}(60→100 °C) = 8.8% can be assigned to the removal of about ten lattice and four coordinating water molecules, respectively. This two-step process matches well with the expected binding behavior of the two types of water molecules in the structure. The lattice water molecules only weakly interact with the MOF, evident from their fast removal kinetics, while the coordinated water molecules interact strongly with Ni^{2+} binding sites, delaying their removal process.

The thermal water removal process was further monitored through powder X-ray diffraction (PXRD) as displayed in **Figure 2c**. After activation of Ni-ZW-MOF at 120 °C for 1 h, the PXRD shows no reflections (blue pattern), indicating the formation of an amorphous phase. It can be assumed that the loss of a combination of lattice and coordinated water molecules leads to structural deformities from the changing coordination environment of Ni^{2+}.[25] Two additional experiments were performed to investigate the MOF's crystallinity upon rehydration. First, the amorphous fully dehydrated sample was exposed to a controlled 80% RH atmosphere for 2 h.

From the respective PXRD (green pattern) it is evident that the sample regains crystallinity although the Bragg reflections do not match to the original as-synthesized phase (red pattern), indicating the formation of a new crystalline phase formed under humid conditions. Second, another dehydrated sample was fully immersed in water for 2 h. The PXRD of the resulting rehydrated sample (magenta pattern) shows reflections matching Bragg positions with the original pristine phase but different reflection intensities, indicating that the dehydration process is reversible. Observing changes in the reflection intensities is no surprise given that the de- and rehydration process causes defects within the macroscopic crystal lattices. Both rehydrated samples were further investigated by TGA showing that the samples from first and second experiments contain about 6.3 (one mass loss step, 13.2%) and 14.4 water molecules/formula unit (two mass loss steps, total 30.4%), respectively. Respective TGA profiles are shown in **Figure S3**.

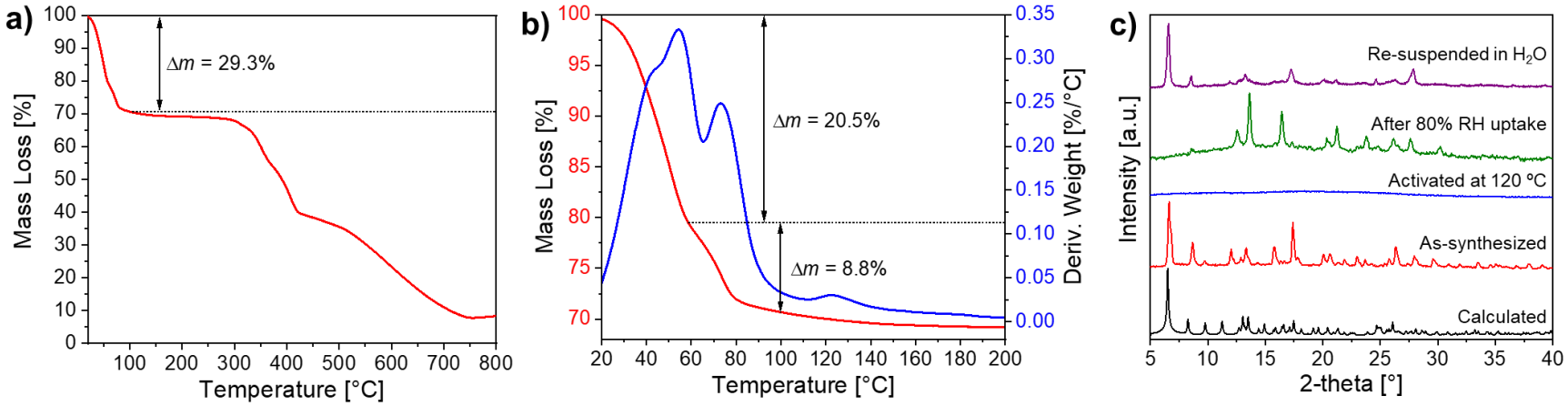

Figure 2. Thermogravimetric and PXRD characterizations of Ni-ZW-MOF. a) Full TGA profile under N_2 atmosphere ranging 20-800 °C; b) TGA (red) and DTG (blue) profiles in the <200 °C range; and c) PXRD analysis after different water adsorption and desorption processes.

Based on the above TGA and PXRD data, the mechanism for thermal activation, water capturing and water harvesting of Ni-ZW-MOF is proposed in **Figure 3**. The thermal activation process occurs in two steps as the as-synthesized material $[Ni(dcpb)(H_2O)_4 \cdot 14H_2O]_n$ first loses the lattice water molecules forming a new crystalline intermediate phase of composition $[Ni(dcpb)(H_2O)_4]_n$ followed by full dehydration to form an amorphous anhydrate of composition $[Ni(dcpb)]_n$. Notably, however, the intermediate phase can only be obtained from partial rehydration of the anhydrate and cannot be directly isolated from thermal activation of the as-synthesized form. Any structural rearrangements during these de- and rehydration processes are best depictable through changes of interchain distances along the crystallographic *c*-axis. For the as-synthesized phase as shown in **Figure 3a**, lattice and metal-coordinating water molecules occupy the interchain voids aiding the formation of a 3D supramolecular interchain framework stabilized by strong intermolecular hydrogen bonding interactions. Followed by full thermal dehydration, all stabilizing H-bonding interactions diminish and consequently all long-range order of the interchain framework collapses leading to the formation of a close and irregular packed amorphous compound as illustrated in **Figure 3b**. Herein, the Ni^{+2} cations act as Lewis acid sites were the water molecules were initially coordinated.[26] Upon exposure to humid air, metal-coordinating water molecules can be reintroduced into the amorphous interchain framework allowing the framework to recrystallize *via* the formation of interchain H-bonding interactions. Given the absence of any lattice water molecules at this stage as depicted in **Figure 3c**, interchain distances of this new crystalline intermediate phase are assumingly shorter as compared to the fully hydrated form. It can be assumed that there is not sufficient critical mass of water molecules in humid air for the sample to return to the as-synthesized phase. However, filling the interchain voids with lattice water molecules becomes possible upon resuspending the sample in water which

eventually transforms the intermediate phase into the as-synthesized form. A similar transformation can be observed when the fully activated anhydrate form is directly resuspended in water. A water adsorption isotherm was obtained to support this mechanism. The isotherm in **Figure S4** shows a two-step adsorption process, corresponding to the coordination of water molecules to the metal center followed by adsorption into the pores at very high relative humidity. The adsorbed water molecules can then be harvested through a thermal reactivation process of the material. As probed below, this process of water capturing and harvesting has the potential to be cycled in order to create a water harvesting system.

During the above experiments, it was observed that Ni-ZW-MOF possesses hydrochromic properties. Previous investigations discussed Ni-ZW-MOF as a photochromic material.[27] Hydrochromic behavior of viologen ligands is infrequently discussed in the literature, owing to the unique and rare occurance.[25,28,29] Hydrochromism occurs as a result of free radical formation *via* electron transfer of the bipyridinium ligand during the dehydration process. Transition metal complexes more commonly exhibit hydrochromic behavior from d-d transitions within the ligand field during the desorption-adsorption process of the water molecules.[25,30–32] The hydrochromic behavior was monitored through diffuse reflectance spectroscopy (DRS) as shown in **Figure 4a**. The as-synthesized Ni-ZW-MOF exhibits a color change from yellow to dark green after thermal activation (**Figure 4b, c**). The color transition can be observed from an increase in the absorbance spectra of the red region (650 nm) between the yellow as-synthesized Ni-ZW-MOF crystals and the green thermally activated material.

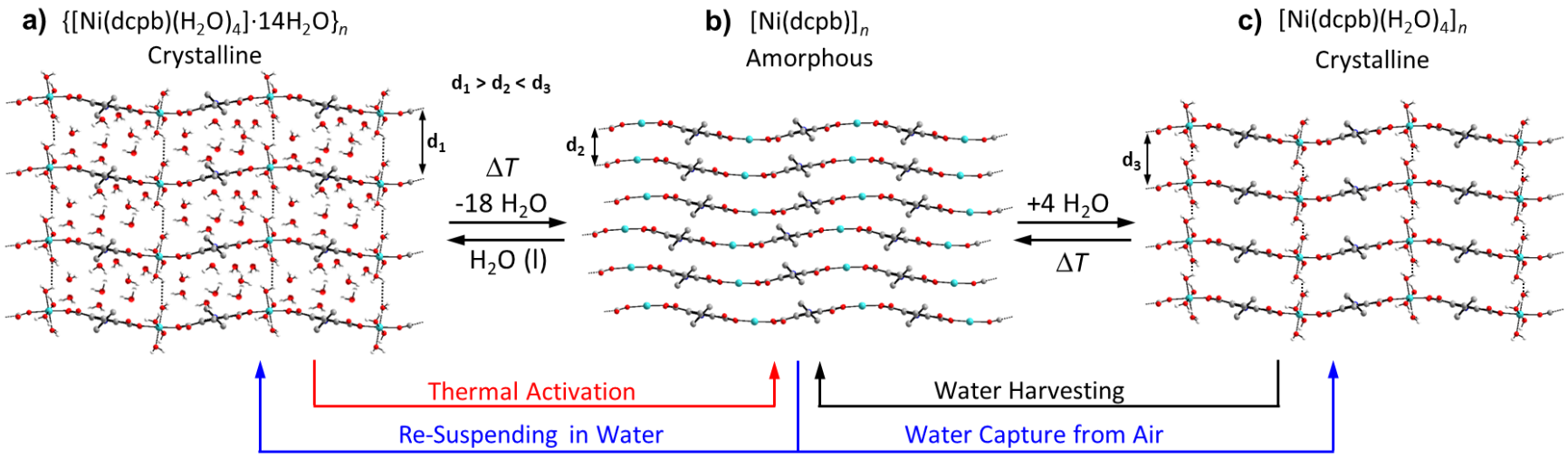

Figure 3. Schematic representation of structural changes during thermal activation, water capturing and water harvesting of Ni-ZW-MOF shown along the crystallographic *c*-axis. Aromatic hydrogens and disorder are omitted for clarity; dashed lines represent H-bonding; grey-carbon, blue-nitrogen, red-oxygen, cyan-nickel.

Based on the hygroscopicity of Ni-ZW-MOF, static and dynamic water adsorption studies were employed to investigate its water harvesting ability. Fixed isothermal adsorption tests were performed on the activated material at 30 °C in four different RH environments (10-80% RH). Per **Figure 4d**, at 10% RH (red curve), an adsorption capacity of 46 mg g^{-1} was observed after exposure to the specified conditions for 90 min. The kinetics of the adsorption process are observed to increase with higher RH, with 40% (blue curve), 50% (cyan curve), and 80% (magenta curve) reaching near full capacity after only 30 min. In addition, at higher RH (50% and 80%), water uptake reaches highest amounts of 151 and 170 mg g^{-1}, respectively, with only a 12% water uptake increase with a 30% RH increase. Given that the expected water uptake between the anhydrate $[Ni(dcpb)]_n$ and the tetra-hydrate intermediate $[Ni(dcpb)(H_2O)_4]_n$ is 136 mg/g, this data suggests that metal-coordinating water molecules are adsorbed below 50% RH and water molecules start filling the pores around 50% RH. Interestingly, this pore filling occurs into the interchain void space of the intermediate phase as depicted in **Figure 3c**. Even at 80% RH the critical mass of water molecules in the gas phase is not sufficient to allow retransformation into the as-synthesized phase as evident from **Figure 2c**, green PXRD. Nevertheless, these findings demonstrate that Ni-ZW-MOF has a strong ability to adsorb water even in low RH conditions.

Similarly, desorption experiments at varying isothermal temperatures and 0% RH were performed after full thermal activation followed by water adsorption at 30 °C and 45% RH. Respective dehydration behavior is plotted in **Figure 4e**. As expected, faster and complete desorption is observed at higher temperatures. For all desorption temperatures tested, desorption kinetics slow down after the first 15 min. Though complete desorption is not achieved at mild desorption temperatures of 30 °C (blue curve), about half of the adsorbed water can be harvested after only 1 h. At 120 °C (black curve), complete desorption was achieved after 45 min of the

isothermal process. These experiments demonstrate that Ni-ZW-MOF is able to function as a water harvesting material under mild conditions—an important prerequisite for designing systems for arid climates.

The recyclability of Ni-ZW-MOF for water harvesting was assessed through dynamic water adsorption-desorption cycling experiments as shown in **Figure 4f** (adsorption conditions: 30 °C and 45% RH; desorption conditions: 80 °C and 0% RH). At mild temperatures, nearly complete desorption was achieved in 90 min (0.5 water molecules/formula unit retained) and over 14 adsorption-desorption cycles, Ni-ZW-MOF retained about 94.2% of its adsorption capacity. The sample's stability after cycling was confirmed by PXRD (**Figure S5**). On average, the observed working capacity of Ni-ZW-MOF is 126.4 mL kg^{-1} $cycle^{-1}$ (3.7 water molecules/formula unit) which outperforms other reported sorbents such as UiO-66 (30 mL kg^{-1}) and Zeolite 13X (20 mL kg^{-1}) under similar conditions.[19]

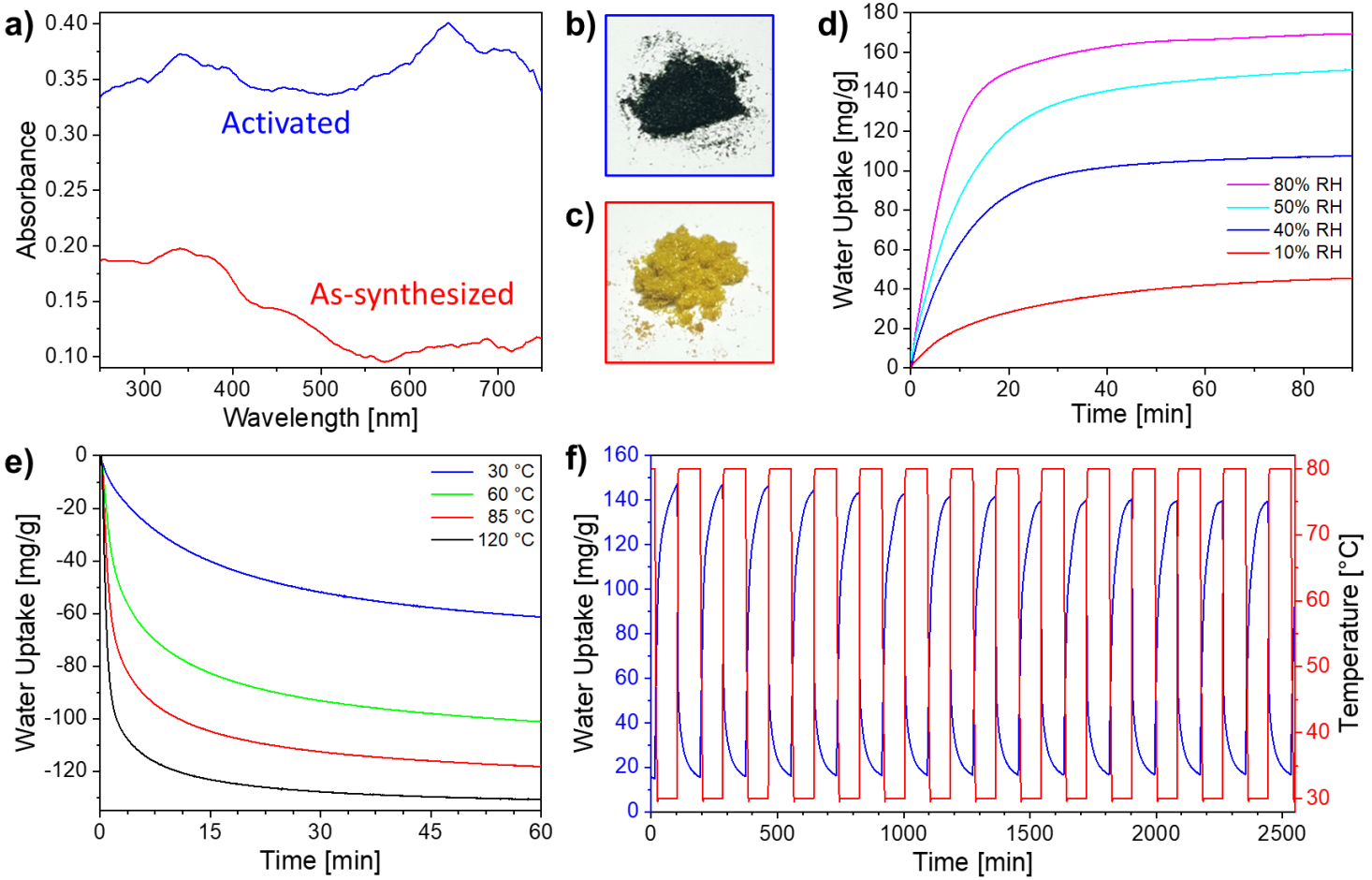

Figure 4. a) DRS spectra of as-synthesized and activated Ni-ZW-MOF; photographs of b) thermally activated and c) as-synthesized Ni-ZW-MOF; d) water adsorption properties at 30 °C and varying % RH (after full thermal activation); e) water desorption properties at varying temperatures and 0% RH (after water adsorption at 30 °C and 45% RH); and f) temperature swing water adsorption-desorption cycles of Ni-ZW-MOF between 30 °C at 45% RH and 80 °C at 0% RH with each isothermal step hold for 90 min.

Conclusions

A Ni(II)-based zwitterionic MOF (Ni-ZW-MOF) was synthesized from a tetratopic disubstituted bipyridinium ligand. The crystal structure features metal-coordinating water molecules in addition to charged-polarized 1D channel pores occupied with lattice water molecules. This water stable MOF can act as Lewis acid when thermally activated due to its open metal sites resulting from the water desorption process along with the pyridinium functionalities of the viologen ligand. When activated, Ni-ZW-MOF can adsorb water from humid air with adsorption capacities of 45.5 mg g^{-1} in 10% RH and 169.5 mg g^{-1} in 80% RH environments. These capacities at low and high RH demonstrate the excellent water harvesting performance of Ni-ZW-MOF. Over multiple adsorption-desorption cycles, Ni-ZW-MOF retained 94.2% of its adsorption capacity, exhibiting an average working capacity of 126.4 mL kg^{-1} $cycle^{-1}$ under given conditions. From the structural features of the MOF one can conclude that the strong Lewis acidity of Ni^{2+} ions and pyridinium moieties accounts for its significant water adsorption capacity. Overall, its stability in aqueous environments and high adsorption performance at low RH, in tandem with low desorption energies and good regeneration abilities, demonstrates the excellent potential for Ni-ZW-MOF as a water harvesting sorbent in arid regions.

Conflicts of Interest

There are no conflicts to declare.

Acknowledgments

M.W. gratefully acknowledges the U.S. National Science Foundation CAREER Program (award no. 1752771) for support of this work.

References

1 P. H. Gleick, Water in Crisis: A Guide to the World's Fresh Water Resources, Oxford University Press, 1993.

2 UN World Water Development Report 2020, https://www.unwater.org/publications/un-world-water-development-report-2020, (accessed 8 November 2022).

3 C. He, Z. Liu, J. Wu, X. Pan, Z. Fang, J. Li and B. A. Bryan, Future global urban water scarcity and potential solutions, Nat. Commun., 2021, 12, 4667. DOI: 10.1038/s41467-021-25026-3

4 A. Boretti and L. Rosa, Reassessing the projections of the World Water Development Report, Npj Clean Water, 2019, 2, 1–6. DOI: 10.1038/s41545-019-0039-9

5 M. T. Kahil, A. Dinar and J. Albiac, Modeling water scarcity and droughts for policy adaptation to climate change in arid and semiarid regions, J. Hydrol., 2015, 522, 95–109. DOI: 10.1016/j.jhydrol.2014.12.042

6 M. Abu-Allaban, A. El-Naqa, M. Jaber and N. Hammouri, Water scarcity impact of climate change in semi-arid regions: a case study in Mujib basin, Jordan, Arab. J. Geosci., 2015, 8, 951–959. DOI: 10.1007/s12517-014-1266-5

7 R. V. Wahlgren, Atmospheric water vapour processor designs for potable water production: a review, Water Res., 2001, 35, 1–22. DOI: 10.1016/S0043-1354(00)00247-5

8 M. Cao, J. Ju, K. Li, S. Dou, K. Liu and L. Jiang, Facile and Large-Scale Fabrication of a Cactus-Inspired Continuous Fog Collector, Adv. Funct. Mater., 2014, 24, 3235–3240. DOI: 10.1002/adfm.201303661

9 A. M. Manokar and A. Karthick, Review on progress in concrete solar water collectors, Environ. Sci. Pollut. Res., 2021, 28, 22296–22309. DOI: 10.1007/s11356-021-13415-6

10 N. Hanikel, M. S. Prévot, F. Fathieh, E. A. Kapustin, H. Lyu, H. Wang, N. J. Diercks, T. G. Glover and O. M. Yaghi, Rapid Cycling and Exceptional Yield in a Metal-Organic

Framework Water Harvester, ACS Cent. Sci., 2019, 5, 1699–1706. DOI: 10.1021/acscentsci.9b00745

11 M. J. Kalmutzki, C. S. Diercks and O. M. Yaghi, Metal–Organic Frameworks for Water Harvesting from Air, Adv. Mater., 2018, 30, 1704304. DOI: 10.1002/adma.201704304

12 W. Xu and O. M. Yaghi, Metal–Organic Frameworks for Water Harvesting from Air, Anywhere, Anytime, ACS Cent. Sci., 2020, 6, 1348–1354. DOI: 10.1021/acscentsci.0c00678

13 L. Wang, K. Wang, H.-T. An, H. Huang, L.-H. Xie and J.-R. Li, A Hydrolytically Stable Cu(II)-Based Metal−Organic Framework with Easily Accessible Ligands for Water Harvesting, ACS Appl. Mater. Interfaces, 2021, 13, 49509–49518. DOI: 10.1021/acsami.1c15240

14 H. Kim, S. R. Rao, E. A. Kapustin, L. Zhao, S. Yang, O. M. Yaghi and E. N. Wang, Adsorption-based atmospheric water harvesting device for arid climates, Nat. Commun., 2018, 9, 1191. DOI: 10.1038/s41467-018-03162-7

15 N. Hanikel, X. Pei, S. Chheda, H. Lyu, W. Jeong, J. Sauer, L. Gagliardi and O. M. Yaghi, Evolution of water structures in metal-organic frameworks for improved atmospheric water harvesting, Science, 2021, 374, 454–459. DOI: 10.1126/science.abj0890

16 H. Kim, S. Yang, S. R. Rao, S. Narayanan, E. A. Kapustin, H. Furukawa, A. S. Umans, O. M. Yaghi and E. N. Wang, Water harvesting from air with metal-organic frameworks powered by natural sunlight, Science, 2017, 356, 430–434. DOI: 10.1126/science.aam8743

17 S. S.-Y. Chui, S. M.-F. Lo, J. P. H. Charmant, A. G. Orpen and I. D. Williams, A Chemically Functionalizable Nanoporous Material [Cu3(TMA)2(H2O)3]n | Science, Science, 1999, 283, 1148–1150. DOI: 10.1126/science.283.5405.1148

18 H. Li, M. Eddaoudi, M. O'Keeffe and O. M. Yaghi, Design and synthesis of an exceptionally stable and highly porous metal-organic framework, Nature, 1999, 402, 276–279. DOI: 10.1038/46248

19 H. Furukawa, F. Gándara, Y.-B. Zhang, J. Jiang, W. L. Queen, M. R. Hudson and O. M. Yaghi, Water Adsorption in Porous Metal–Organic Frameworks and Related Materials, J. Am. Chem. Soc., 2014, 136, 4369–4381. DOI: 10.1021/ja500330a

20 X. Liu, X. Wang and F. Kapteijn, Water and Metal–Organic Frameworks: From Interaction toward Utilization, Chem. Rev., 2020, 120, 8303–8377. DOI: 10.1021/acs.chemrev.9b00746

21 F. Jeremias, V. Lozan, S. K. Henninger and C. Janiak, Programming MOFs for water sorption: amino-functionalized MIL-125 and UiO-66 for heat transformation and heat storage applications, Dalton Trans., 2013, 42, 15967–15973. DOI: 10.1039/C3DT51471D

22 H. Reinsch, M. Feyand, T. Ahnfeldt and N. Stock, CAU-3: A new family of porous MOFs with a novel Al-based brick: [Al2(OCH3)4(O2C-X-CO2)] (X = aryl), Dalton Trans., 2012, 41, 4164–4171. DOI: 10.1039/C2DT12005D

23 D. Aulakh, J. R. Varghese and M. Wriedt, A New Design Strategy to Access Zwitterionic Metal–Organic Frameworks from Anionic Viologen Derivates, Inorg. Chem., 2015, 54, 1756–1764. DOI: 10.1021/ic5026813

24 D. Aulakh, A. P. Nicoletta, J. R. Varghese and M. Wriedt, The structural diversity and properties of nine new viologen based zwitterionic metal–organic frameworks, CrystEngComm, 2016, 18, 2189–2202. DOI: 10.1039/C6CE00284F

25 J. Liu, Y. Lu and W. Lu, Photochromism and hydrochromism of three two-dimensional coordination polymers constructed from a carboxybenzyl viologen ligand, Dyes Pigments, 2020, 182, 108631. DOI: 10.1016/j.dyepig.2020.108631

26 A. Leblanc, N. Mercier, M. Allain, M.-C. Dul, G. Weber, N. Geoffroy, J.-P. Bellat and I. Bezverkhyy, A robust viologen and Mn-based porous coordination polymer with two types of Lewis acid sites providing high affinity for H2O, CO2 and NH3, Dalton Trans., 2017, 46, 15666–15670. DOI: 10.1039/C7DT03541A

27 J.-J. Liu, T. Liu, S.-B. Xia, F.-X. Cheng and C.-C. Huang, Synthesis, crystal structures and photochromic properties of two coordination polymers based on a rigid tetracarboxylic acid ligand, Transit. Met. Chem., 2017, 42, 525–531. DOI: 10.1007/s11243-017-0157-5

28 C. Zhang, L. Sun, Y. Yan, H. Shi, B. Wang, Z. Liang and J. Li, A novel photo- and hydrochromic europium metal–organic framework with good anion sensing properties, J. Mater. Chem. C, 2017, 5, 8999–9004. DOI: 10.1039/C7TC03013D

29 Q. Sui, X.-T. Ren, Y.-X. Dai, K. Wang, W.-T. Li, T. Gong, J.-J. Fang, B. Zou, E.-Q. Gao and L. Wang, Piezochromism and hydrochromism through electron transfer: new stories for viologen materials, Chem. Sci., 2017, 8, 2758–2768. DOI: 10.1039/C6SC04579K

30 T. Zheng, J. M. Clemente-Juan, J. Ma, L. Dong, S.-S. Bao, J. Huang, E. Coronado and L.-M. Zheng, Breathing Effect in a Cobalt Phosphonate upon Dehydration/Rehydration: A Single-Crystal-to-Single-Crystal Study, Chem. – Eur. J., 2013, 19, 16394–16402. DOI: 10.1002/chem.201302514

31 X.-D. Yang, R. Zhu, J.-P. Yin, L. Sun, R.-Y. Guo and J. Zhang, Bipyridinium-Bearing Multi-stimuli Responsive Chromic Material with High Stability, Cryst. Growth Des., 2018, 18, 3236–3243. DOI: 10.1021/acs.cgd.8b00390

32 K. Uemura, S. Kitagawa, M. Kondo, K. Fukui, R. Kitaura, H.-C. Chang and T. Mizutani, Novel flexible frameworks of porous cobalt(II) coordination polymers that show selective guest adsorption based on the switching of hydrogen-bond pairs of amide groups, *Chem. - Eur. J.*, 2002, **8**, 3586–3600. DOI: 10.1002/1521-3765(20020816)8:16<3586::AID-CHEM3586>3.0.CO;2-K